Bioprocess Biosyst Eng (2016) 39:1923–1931
DOI 10.1007/s00449-016-1666-x

ORIGINAL PAPER

Antibacterial, anti-biofilm and anticancer potentials of green synthesized silver nanoparticles using benzoin gum (*Styrax benzoin*) extract

Juan Du[1] · Hina Singh[1] · Tae-Hoo Yi[1]

Received: 7 June 2016 / Accepted: 2 August 2016 / Published online: 5 August 2016

Abstract This study described a simple and green approach for the synthesis of silver nanoparticles (AgNPs) employing benzoin gum water extract as a reducing and capping agent and their applications. The AgNPs were characterized by ultraviolet–visible spectrophotometer, X-ray diffraction pattern, field emission transmission electron microscopy, dynamic light scattering, zeta potential and fourier transform infrared spectroscopy. The AgNPs showed promising antimicrobial activity against various pathogens (Gram-negative, Gram-positive and fungus) and possessed high free radical scavenging activity (104.5 ± 7.21 % at 1 mg/ml). In addition, the AgNPs exhibited strong cytotoxicity towards human cervical cancer and human lung cancer cells as compared to the normal mouse macrophage cells. Moreover, the AgNPs possessed anti-biofilm activity against *Escherichia coli*, and compatibility to human keratinocyte HaCaT cells, which suggests the use of dressing with the AgNPs in chronic wound treatment. Therefore, AgNPs synthesized by benzoin gum extract are comparatively green and may have broad spectrum potential application in biomedicine.

✉ Tae-Hoo Yi
drhoo@khu.ac.kr

Juan Du
bio.dujuan@hotmail.com

Hina Singh
hina@khu.ac.kr

[1] Department of Oriental Medicinal Biotechnology, College of Life Science, Kyung Hee University, Global Campus, 1732 Deokyoungdaero, Giheung-gu, Yongin-si, Gyeonggi-do 446-701, Republic of Korea

Keywords Benzoin gum · Biosynthesis · Silver nanoparticles · Antibacterial · Anti-biofilm · Cytotoxicity

Introduction

Nanoparticles (NPs) cause attraction of researchers because of their unique properties, owing to their small size (1–100 nm), large surface-to-volume ratio and increased reactivity [1]. Specifically, AgNPs play a significant role in the field of biology and medicine, and have been commonly used as antimicrobial and antifungal agents for a wide variety of products, such as medical dressing, packaging, cosmetics, paints, spray and textile fabrics and toothbrushes [2]. Generally, AgNPs are prepared by chemical methods which are usually carried out at high temperatures with chemical reducing agents [3, 4]. During the chemical synthesis process, reducing agent donates electrons to the Ag^{+}, resulting in reverting Ag^{+} to Ag^{0}. The biological approaches of synthesis AgNPs employing plant extracts and microorganisms is termed as economic and environmental friendly biomaterial and received tremendous attention [5]. The active ingredients contained in plant extracts act as reducing agents. It is found that the catalytic and antibacterial properties of AgNPs depend on their size, shape and capping agents [6, 7]. Reducing agents, reaction media, temperature and Ag precursors influence the size and shape of AgNPs, since they define the pressure of the reaction. If the reaction pressure is high, the process of nucleation and growth of the nanoparticles is greatly accelerated, and the opposite effect will occur at low pressure, causing various shapes and sizes of synthesized AgNPs.

Human beings and animals are often infected by pathogenic microorganisms in the living environment,

and the marked increased resistance of pathogen to antibiotics in the past two decades is a growing concern for doctors and medical officials world-wide [8]. One of the modes by which bacteria exert this persistent infections resistant to systemic antibiotic therapy is their ability to develop biofilms [9]. Biofilms are bacterial communities encased in a self-produced extracellular polymeric substance (EPS) to create more complex structures [10]. Chronic wounds are a severe worldwide problem, and they are ideal environment for bacterial colonization. Compared to planktonic cells biofilm cells may play an important role, causing infection of both acute and chronic wounds. Around 60 % of chronic wounds contain biofilms, which represent a challenge to the treatment [11]. The AgNPs have a broad antibacterial activity, and have been commonly used as an essential additive in number of products such as medical dressing, packaging, cosmetics, paints, spray and textile fabrics for their inhibitory effects on microbes [2]. Apart from the antimicrobial properties, AgNPs exhibit a cytotoxic behavior to normal and cancer cells. Considering this, in this study we aim to find a fast, simple and nontoxic strategy to synthesis the AgNPs which exhibit anti-biofilm activity and have low cytotoxic effects and generate a better biocompatibility to normal cells.

Benzoin gum is a balsam obtained from *Styracaceae* trees of the family *Styracaceae* and produced mainly in Asia [12]. Benzoin gum has been widely used in flavor and fragrance industry owing to its pleasant, sweet balsamic odor, and also is used in pharmaceutical and traditional Chinese medicine preparations as an ingredient and carrier [13]. The main constituents of benzoin gum are coniferyl benzoate, benzoic acid, *p*-coumaryl benzoate, cinnamyl cinnamate, vanillin and siaresinolic acid [13, 14]. In this study, we synthesized the AgNPs by benzoin gum water extract, evaluate the ability of antibacterial and antibiofilm of the AgNPs and their compatibility with human keratinocyte HaCat cells, for its possible application in chronic wounds; and evaluate their cytotoxic effects in human cervical cancer cells, human lung cancer cells and mouse macrophage cells, for its possible application in cancer treatment.

Materials and methods

Materials

Silver nitrate ($AgNO_3$), crystal violet solution, MTT, dimethyl sulfoxide (DMSO), methanol, DPPH and sodium bicarbonate were purchased from Sigma-Aldrich (St. Louis, USA). Fetal bovine serum (FBS), Dulbecco's modified eagle medium (DMEM), and penicillin–streptomycin were purchased from Gibco BRL (Grand Island, NY, USA). Raw 264.7 (mouse macrophage), Hela (human cervical cancer), A549 (human lung cancer) and HaCaT (human keratinocyte) cells were employed from Korean Cell Line Bank (KCLB, Seoul, Korea). Media used for bacterial cultures were procured from Oxoid Ltd. (Basingstoke, England). Benzoin gum powder (*Styrax benzoin*), which purchased form Mountain Rose Herbs (Eugene, Oregon, USA), was originally harvested from Indonesia. The pathogenic bacterial cultures *Candida tropicalis* ATCC 18807, *Pseudomonas aeruginosa* ATCC 10145, *E. coli* ATCC 43894 and *Staphylococcus aureus* ATCC 6538 were purchased from American Type Culture Collection (ATCC, Manassas, VA, USA).

Preparation of the benzoin gum extract and synthesis of AgNPs

50 g of benzoin gum powder was boiled in a conical flask containing 500 ml of deionized water for 20 min. The water extract was centrifuged, supernatant obtained was filtered through a 0.45 μm PVDF syringe filter (SmartPor, Seoul, Korea). Then, aqueous solution of $AgNO_3$ at a final concentration of 1 mM was added to the extract. The mixture was stirred on a magnetic stirrer at 60 °C. The synthesis of AgNPs was indicated by color change of the reaction mixture. The AgNPs were collected by high speed centrifugation at 22,000 rpm for 30 min. The pellet obtained was washed thoroughly and air dried for characterization and further studies.

Characterization of the AgNPs

The morphology of the AgNPs was analyzed using FE-TEM (JEM-2100F, JEOL, Tokyo, Japan), operated at a voltage of 200 kV. UV–vis spectrums of the AgNPs were recorded between the wavelength range from 300 to 800 nm (Optizen POP; Mecasys, Daejeon, Korea). The functional groups capped on surface of the AgNPs were identified using a FTIR spectroscopy (Spectrum One System, Perkin-Elmer, Waltham, MA, USA). Benzoin gum water extract powder was prepared and performed FTIR. The hydrodynamic size and zeta potential of the AgNPs were investigated by DLS analysis using a Malvern Zetasizer Nano ZS90 (Malvern Instruments, Worcestershire, UK). The selected-area electron diffraction (SEAD) and XRD (D8 Advance, Karlsruhe, Bruker) were used to detect the crystal structure of the synthesized AgNPs. Moreover, energy dispersive X-ray spectroscopy (EDX) and elemental mapping of the AgNPs were performed.

Antimicrobial testing

Disk diffusion method on Mueller–Hinton agar (MHA) plates was used to determine the antimicrobial activity of the AgNPs. Briefly, 100 µl fresh overnight inoculums of *C. tropicalis*, *E. coli*, *S. aureus* and *P. aeruginosa* cultures were spread on MHA plates. The sterile paper discs of 8 mm in diameter loaded with 30 µl of the AgNPs (500 and 1000 ppm) were placed on the surface of the inoculated plates. The plates were incubated for 24 h at 33 °C and the inhibition zone (diameter in mm) of each well was measured. The assay was carried out in triplicate for all the test organisms.

Anti-biofilm testing

The anti-biofilm activity of the AgNPs was determined by colorimetric method against strain *E. coli*. Fresh overnight inoculum of *E. coli* (400 µl/well) was added in triplicate to wells of 48-well tissue culture plates (SPL Lifescience, Pocheon, Korea). Biofilms were formed after culturing for 48 h, the medium were removed from the wells and different concentrations of the AgNPs ranging from 1 to 10 µg/ml in sterile water were added to the wells, sterile water were used as control. After 24 h incubation at 33 °C, the solutions were removed and wells were washed with sterile water. The plates were air dried for 1 h and 400 µl of 1 % (v/v) crystal violet solution were added in each well and incubated for 30 min. Thereafter, the crystal violet solution was removed and wells were washed with sterile water. For the quantification of adherent cells, the crystal violet was solubilized with 200 µl of 95 % (v/v) ethanol. A FilterMax F5 Microplate Reader (Molecular Devices, Sunnyvale, CA, USA) was used to measure the absorbance at 575 nm. The effect of the AgNPs was expressed as the biofilm formation %, using the following formula: biofilm formation % $= \text{Abs}_{\text{treated}}/\text{Abs}_{\text{control}} \times 100$.

Antioxidant assay

Free radical scavenging activity was determined by DPPH assay. 20 µl of different concentrations of the AgNPs were placed in a 96-well plate, 180 ml of DPPH (0.2 mM) in methanol was also added. DPPH solution without silver nanoparticles served as the blank. Control was prepared as above solutions without AgNPs. The plate was standing at 37 °C for 30 min, and the absorbance was measured by the Microplate Reader at wavelength of 520 nm. Arbutin was used as positive control. The effect of the AgNPs was expressed as DPPH radical scavenging activity %, using the following formula: scavenging capacity % $= 100 - [(\text{Abs}_{\text{sample}} - \text{Abs}_{\text{blank}})/\text{Absorbance}_{\text{control}}] \times 100$. The study was done in triplicate.

Cell culture and MTT assay

The cytotoxicity of the AgNPs on HaCaT, Raw 264.7, Hela and MCF-7 cells was studied. Cells were maintained in DMEM medium supplemented with 1 % penicillin–streptomycin and 10 % FBS at 37 °C in a humidified atmosphere containing 5 % CO_2. Stock solution of AgNPs was prepared in sterile deionized water and diluted using the medium (without FBS). HaCaT Cells (2×10^3/well) and Raw 264.7, Hela and MCF-7 cells (10^4/well) in 0.2 ml medium/well were plated in triplicate in 96 well cell culture plates (SPL Lifescience, Pocheon, Korea) and incubated for 72 h. Cells were treated with different concentrations of the AgNPs and incubated for a further 24 h, non-treated cells were used as control. Following the incubation, MTT at a final concentration of 0.1 mg/ml was added to each well and further incubated for 3 h. Viable cells were determined by measuring UV absorption at 570 nm. The effect of the AgNPs was expressed as the cell viability %, using the following formula: cell viability % $= \text{Abs}_{\text{treated cells}}/\text{Abs}_{\text{control cells}} \times 100$.

Results and discussion

Characterization of the AgNPs

The color of benzoin gum extract was changed from clear to deep brown within 5 h (Fig. 1a, b), indicated the formation of AgNPs, as a result of the surface plasmon resonance phenomenon [15]. UV–Vis spectra of the mixture were shown in Fig. 1c and d, a peak at around 450 nm was observed, confirmed the formation of the AgNPs. Using DLS, the AgNPs in aqueous solution showed a narrow size distribution ranging from 12 to 38 nm, average hydrodynamic size and zeta potential were observed to be 18.7 ± 1.2 nm and -27.1 ± 0.5 mV, respectively (Fig. 1d, e). The zeta potential value gave an important idea regarding surface charge and indicated that the AgNPs were stable and discrete in aqueous solution. FE-TEM images revealed the majorities of the AgNPs formed were spherical in shape (Fig. 2a, b). The SAED pattern (Fig. 2c) showed four rings which can be indexed to (111), (200), (220) and (311) lattice planes of face-centered cubic silver, respectively. In the XRD pattern (Fig. 3) of the AgNPs, diffraction peaks at 2θ values of 38.05°, 44.17°, 64.42° and 77.31° were identified and matched with JCPDS databases of the standard silver (file No. 04-0783). Those 2θ values can be indexed to respective (111), (200), (220) and (311) diffraction planes, in line with the result of SAED. The elemental mapping (Fig. 4a, b) and EDX (Fig. 4c) showed the distribution of silver element and characteristic signals of silver atoms, respectively. The presence of signals of

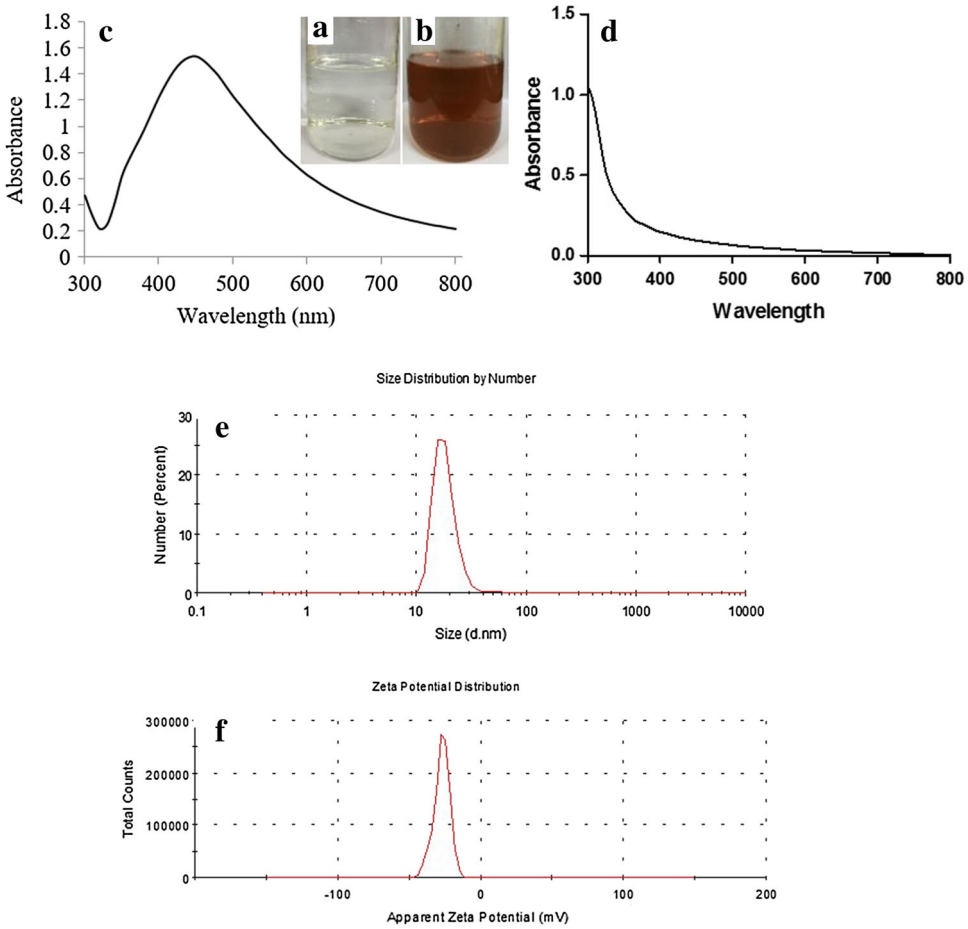

Fig. 1 Digital images of benzoin gum extract (**a**) and the synthesized silver nanoparticles (**b**); UV–vis spectra of the AgNPs (**c**) and the control which contains benzoin gum extract and $AgNO_3$, DLS (**d**) and surface zeta potential (**e**) result

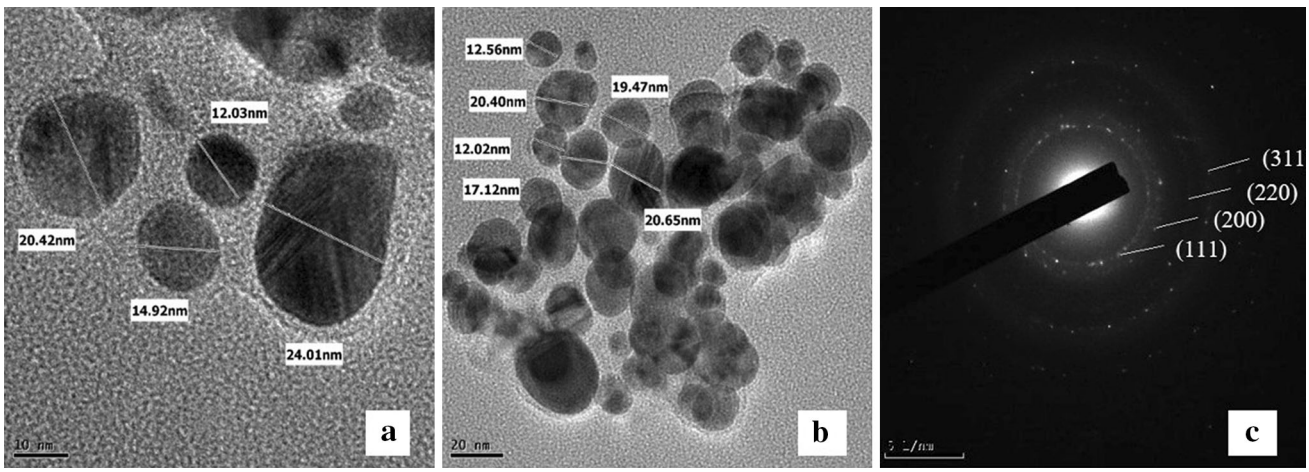

Fig. 2 FE-TEM images (**a**, **b**), and SAED pattern (**c**) of the synthesized AgNPs

copper and carbon in EDX was because of the use of FE-TEM grid [16].

The FTIR spectrum obtained from benzoin gum water extract powder and the AgNPs were shown in Fig. 5a and b, respectively. The broad peak around 3419 and 3421 cm^{-1} can be assigned to O–H stretching vibration of functional groups [17]. The peaks around 2957 and 2872, 2923 and 2852/cm is attributed to C–H asymmetric and symmetric stretching vibration of methylene [18]. The minor as well as sharp peak at 1642/cm is due to C=C stretching vibration of alkenyl groups in benzoin gum extract [19]. The peaks at 1598 and 1583/cm is attributed to

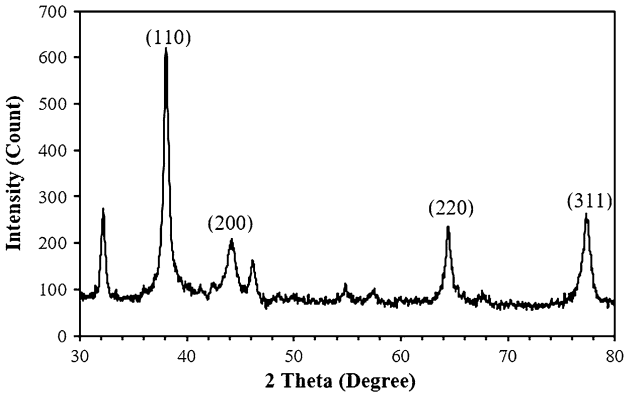

Fig. 3 XRD spectra of synthesized AgNPs

C=C–C stretching vibration of aromatic rings [20]. The peak around 1558/cm can be assigned to carboxylate group stretching vibration. The band observed at 1451/cm is due to C–H stretching vibration of methylene bridge [21]. The strong band observed at 1411/cm is attributed to C–H stretching vibration of vinyl [22]. Additionally, the broad peak around 1070 and 1077/cm can be assigned to C–O–C stretching vibration [23]. Among them, the peaks of 1642 and 1558/cm in benzoin gum extract lost intensity in the AgNPs, band 1450/cm is shifted to 1376/cm, and band 1441/cm is shifted to 1207/cm, which indicate the involvement of the corresponding groups mentioned above during the reduction of Ag^{+} to Ag^{0}, suggesting the role of coniferyl benzoate and *p*-coumaryl benzoate in the synthesis of the AgNPs.

Antibacterial activity of the AgNPs

AgNPs were known for the capable of antimicrobial activity, to overcoming the limited resource of antibiotics, AgNPs had been studied and shown the potential as a new generation of antimicrobials [24]. In this study, antimicrobial activity of the AgNPs were tested against a range of pathogenic microorganisms including Gram-positive *S. aureus*, Gram-negative *E. coli*, *P. aeruginosa*, and fungal strain *C. tropicalis* (Fig. 6). The inhibition zones of the AgNPs against pathogenic strains are shown in Table 1.

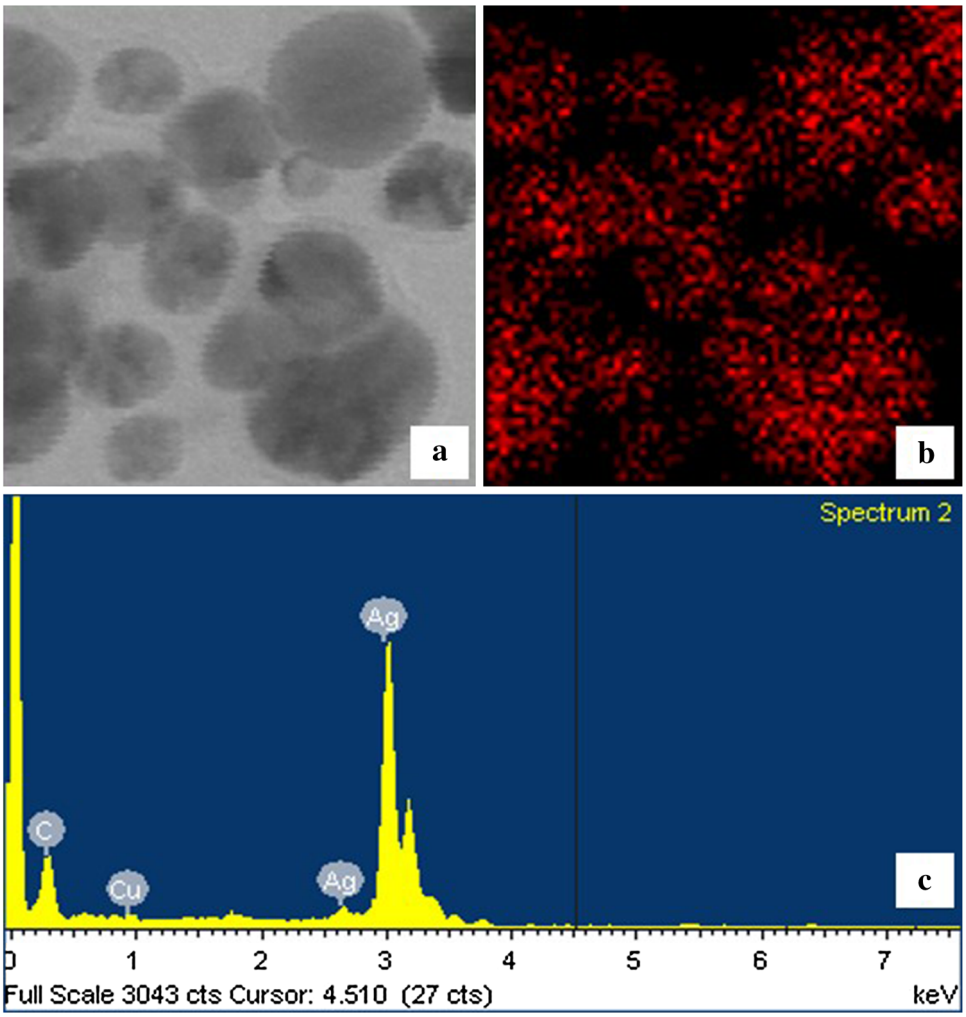

Fig. 4 The elemental mapping of synthesized AgNPs: TEM image used for mapping (**a**) and silver distributions (**b**); EDX spectrum of synthesized AgNPs (**c**)

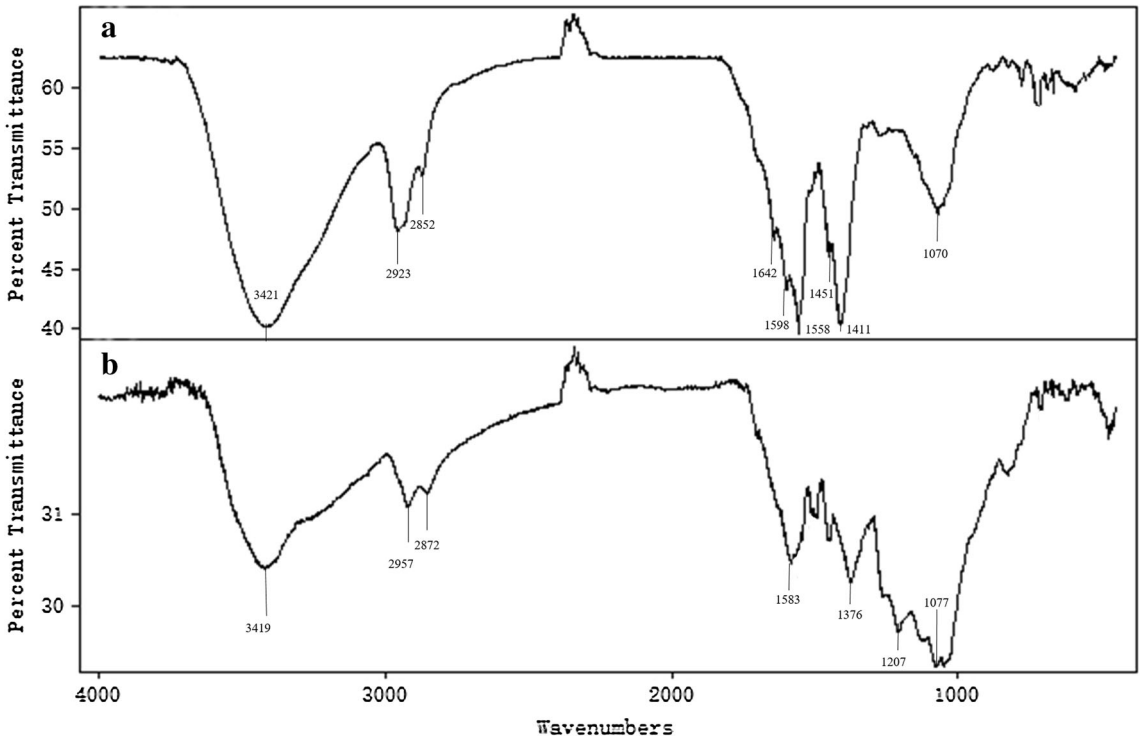

Fig. 5 FTIR spectrum of benzoin gum water extract powder (*a*) and the AgNPs (*b*)

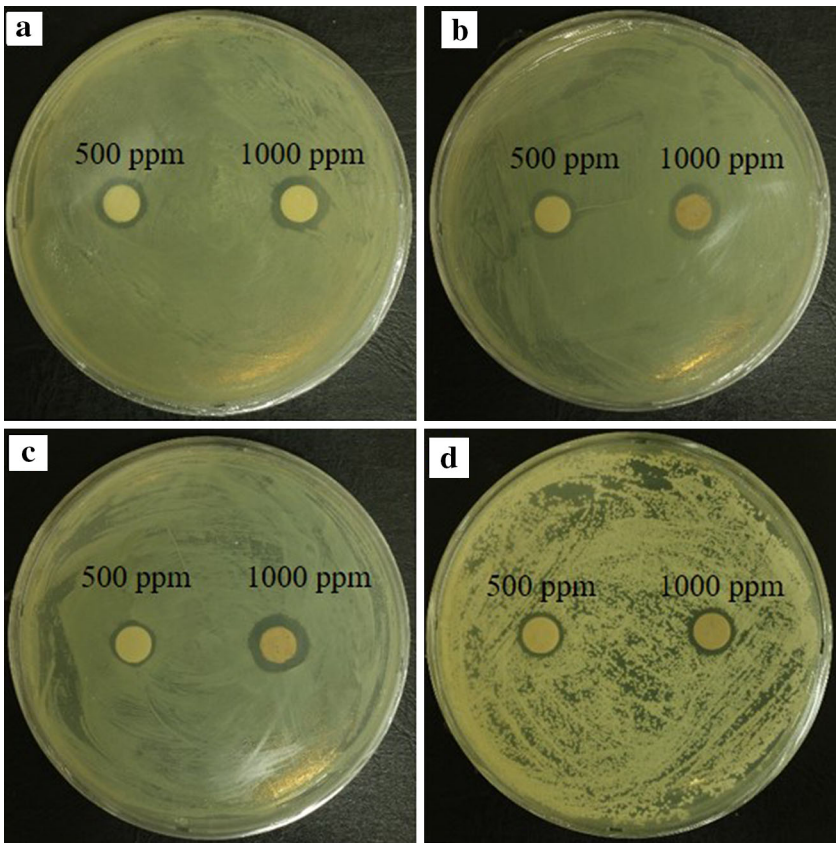

Fig. 6 Antimicrobial activities of synthesized AgNPs (30 µl) at 500 and 1000 ppm concentrations in water against *P. aeruginosa* (**a**), *S. aureus* (**b**), *E. coli* (**c**) and *C. tropicalis* (**d**)

Table 1 Antimicrobial activity of the AgNPs against selected pathogenic strains

Pathogenic microorganism	Zone of inhibition (mm)	
	AgNPs (500 ppm)	AgNPs (1000 ppm)
P. aeruginosa	11.0 ± 0.7	12.6 ± 0.6
S. aureus	9.9 ± 0.5	11.7 ± 0.6
E. coli	9.5 ± 0.5	13.7 ± 0.3
C. tropicalis	9.3 ± 0.6	10.6 ± 0.4

The experiments were done in triplets and the results were interpreted in terms of standard deviation of mean diameter of zone of inhibition

The results indicated that the antibacterial activity ability of AgNPs against all the tested bacterial strains, and the activity was increased with the increasing of AgNPs concentrations.

Anti-biofilm assay

The majority of the bacteria in natural habitats live as biofilms, which have up to 1000 times more resistant to antimicrobial agents than those in a planktonic state [25]. However, most of the antibiotics and the methods for antimicrobial work have been developed for planktonic bacteria. There is a great need to meet the demands of effective anti-biofilm therapy. Herein, we studied the effect of AgNPs on biofilm formation of strain *E. coli* with respect to wide distribution of the strain. *E. coli* grown in wells were treated with concentrations of AgNPs ranging from 1 to 10 μg/mL. Treatment for 24 h resulted in approximately 10.9, 44.1, 54.0 and 65.5 % decrease in biofilm formation at 1, 2, 5 and 10 μg/mL concentration, respectively (Fig. 7a), indicate that the AgNPs were able to inhibit the biofilm formation of *E. coli.*

Cytotoxic effect of the AgNPs

Despite of its excellent antibacterial and anti-biofilm activities, the potential biological applications of AgNPs were limited due to their cytotoxicity against human cells. Therefore, we checked the cytotoxic effect of the AgNPs on human keratinocyte HaCaT cells. The AgNPs exhibited no significant cytotoxic effect up to 10 μg/mL concentration (Fig. 7b). This good biocompatibility indicated that the AgNPs display anti-biofilm activity without being harmful to human keratinocyte HaCat cells at this concentration, and were further able to be used for prevention and treatment of bacterial infections in chronic wounds.

The anticancer activity of the AgNPs was evaluated by cytotoxicity on Raw 264.7 (non-cancerous), Hela (human cervical cancer) and A549 (human lung cancer), at different concentrations (1, 2, 5 μg/mL). The AgNPs exhibited biocompatible nature with Raw 264.7 cells at low concentrations (1 and 2 μg/mL); however, they were found to be cytotoxic to A549 and Hela in a dose dependent manner under identical culture conditions (Fig. 8). The cell viability % of Hela and A549 cells was decreased to 54 ± 3.85 and 40.0 ± 2.45 %, respectively, after treatment with AgNPs at quite low concentration of 1 μg/ml. The cell viability of Raw 264.7, Hela and A549 cells was decreased to 56.4 ± 5.7, 40.5 ± 5.3 and 44.8 ± 2.4 %, respectively, after the concentration increased to 5 μg/mL. These results in this study indicated that the AgNPs may have potential as inhibitors of Hela and A549 cells growth in low concentrations. AgNPs are known to be cytotoxic to cancer cells, through the various mechanisms [26, 27]. Recently reports suggested that the generation of ROS play a pivotal role in the AgNPs induced cytotoxicity in cancer cells. The possible mechanisms is AgNPs trigger intracellular ROS by inhibiting the synthesis of intracellular antioxidant systems, and the generated ROS favors the DNA damage leading to cell death [28, 29]. According to this, the free radical scavenging activity of the AgNPs may contribute to the cytotoxicity against A549 and Hela cells. The low cytotoxic effect of the synthesized AgNPs against Raw 264.7 and HaCaT cells may because of the functional groups capped on surface of the AgNPs, those groups may biocompatibility and low toxicity. Thus, the AgNPs could be a good candidate for the treatment of the cancer cells via cytotoxic mechanisms.

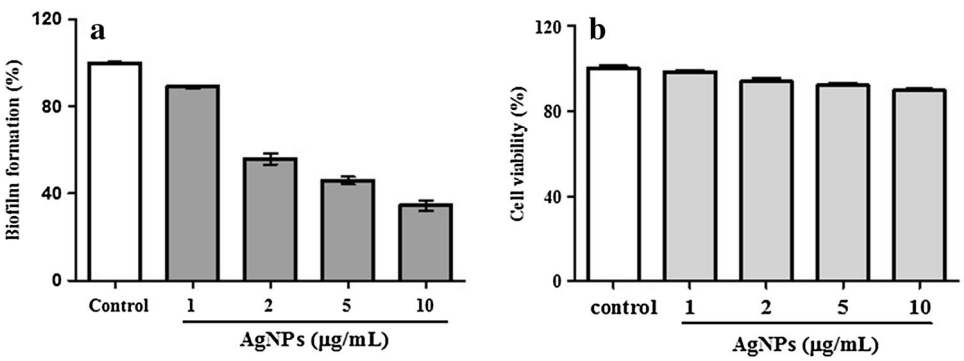

Fig. 7 Effect of AgNPs on biofilm formation of strain *E. coli* (**a**), MTT cytotoxicity assay of AgNPs against human keratinocyte HaCat cells (**b**). Experiments were performed in triplicates; mean ± SD are shown

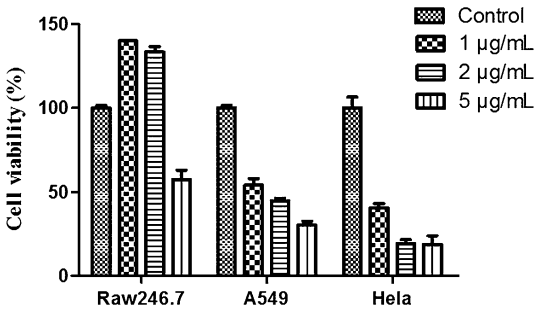

Fig. 8 MTT cytotoxicity assay of AgNPs against Raw 264.7, A549 and Hela cell lines (values are mean ± SD of three determinations)

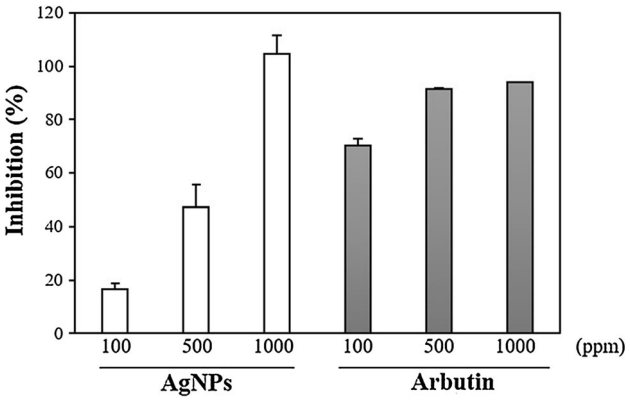

Fig. 9 DPPH free radical scavenging assay of AgNPs and arbutin (values are mean ± SD of three determinations)

Antioxidant efficacy of the AgNPs

Reactive oxygen species (ROS) are highly reactive oxidant molecules that are forms as natural byproduct during the body's metabolic reactions, the dramatically increase of reactive oxygen species may result in significant damage to cell structures [30, 31]. Antioxidants are the substances which can scavenge free radicals and prevent and repair damages caused by ROS, therefore, can decrease the risk of cancer and degenerative diseases [32]. The antioxidant activity of the AgNPs was detected by DPPH assay in the different concentration of 100, 500 and 1000 μg/ml. A freshly prepared DPPH solution showed deep purple color with the absorption maxima at 517 nm, and the presence of an antioxidant in the medium lead to disappearance of the purple color [33]. Arbutin was used as a positive control. In this study, the AgNPs possessed free radical scavenging activity (Fig. 9), which increased in a dose-dependent manner. The tested scavenging ability for the lowest concentration of the AgNPs (100 μg/ml) was 16.66 ± 2.18 % and the inhibition capacity was increased to 104.50 ± 7.21 % at the concentration of 1000 μg/ml. The IC50 values for AgNPs was found to be 471.13 ± 6.7 μg/ml. The synthesized AgNPs were found to be potent free radical scavenger. These results indicate that the AgNPs could work as potent antioxidants.

Conclusion

Synthesis of AgNPs using benzoin gum extract is an ecofriendly and relatively new manner. The synthesized AgNPs were characterized by several instrumental techniques, and the efficacy of the AgNPs was further studied. The AgNPs showed excellent antimicrobial ability against all the tested pathogenic strains. The AgNPs exhibited the anti-biofilm activity, and the cell viability studies in human keratinocyte HaCat cells showed good biocompatibility at concentrations up to 10 μg/ml, suggesting its potential application as an agent in chronic wound healing. In addition, the AgNPs possessed antioxidant property and remarkable toxicity to Hela and A549 cells even at concentrations of 1 μg/ml, suggesting its possible use anticancer agent. However, further researches are needed to study the mechanism and develop the technology into therapeutic and preventive strategies.

Acknowledgments This work was conducted under the industrial infrastructure program (No. N0000888) for fundamental technologies which is funded by the Ministry of Trade, Industry & Energy (MOTIE, Korea).

Compliance with ethical standards

Conflict of interest The authors declare that they have no competing interests.

References

1. Zhang L, Wang X, Miao Y, Chen Z, Qiang P, Cui L, Jing H, Guo Y (2016) Magnetic ferroferric oxide nanoparticles induce vascular endothelial cell dysfunction and inflammation by disturbing autophagy. J Hazard Mater 304:186–195
2. Lara HH, Garza-Trevino EN, Ixtepan-Turrent L, Singh DK (2011) Silver nanoparticles are broad-spectrum bactericidal and virucidal compounds. J Nanobiotechnol 9:30
3. Jayaprakash N, Vijaya JJ, Kennedy LJ, Priadharsini K, Palani P (2015) Antibacterial activity of silver nanoparticles synthesized from serine. Mater Sci Eng C Mater Biol Appl 49:316–322
4. Mishra PM, Sahoo SK, Naik GK, Parida K (2015) Biomimetic synthesis, characterization and mechanism of formation, of stable silver nano particles using *Averrhoa carambola* L. leaf extract. Mater Lett 160:566–571
5. Otari SV, Patil RM, Ghosh SJ, Pawar SH (2014) Green phytosynthesis of silver nanoparticles using aqueous extract of *Manilkara zapota* (L.) seeds and its inhibitory action against Candida species. Mater Lett 116:367–369
6. Lu Z, Rong K, Li J, Yang H, Chen R (2013) Size-dependent antibacterial activities of silver nanoparticles against oral anaerobic pathogenic bacteria. J Mater Sci Mater Med 24:1465–1471

7. Xu R, Wang D, Zhang J, Li Y (2006) Shape-dependent catalytic activity of silver nanoparticles for the oxidation of styrene. Chem Asian J 1:888–893
8. Ahamed M, Alsalhi MS, Siddiqui MK (2010) Silver nanoparticle applications and human health. Clin Chim Acta 411:1841–1848
9. Danese PN (2002) Antibiofilm approaches: prevention of catheter colonization. Chem Biol 9:873–880
10. Perez-Diaz M, Alvarado-Gomez E, Magana-Aquino M, Sanchez-Sanchez R, Velasquillo C, Gonzalez C, Ganem-Rondero A, Martinez-Castanon G, Zavala-Alonso N, Martinez-Gutierrez F (2016) Anti-biofilm activity of chitosan gels formulated with silver nanoparticles and their cytotoxic effect on human fibroblasts. Mater Sci Eng C Mater Biol Appl 60:317–323
11. Clinton L, Carter T (2015) Chronic wound biofilms: pathogenesis and potential therapies. Labmedicine 46:277–284
12. Filippi JJ, Castel C, Fernandez X, Rouillard M, Gaysinski M, Lavoine-Hanneguelle S (2009) An unusual acenaphthylene-type sesquiterpene hydrocarbon from Siam and Sumatra benzoin gum. Phytochem Lett 2:216–219
13. Castel C, Fernandez X, Lizzani-Cuvelier L, Loiseau AM, Perichet C, Delbecque C, Arnaudo JF (2006) Volatile constituents of benzoin gums: Siam and Sumatra, part 2. Study of headspace sampling methods. Flavour Fragr J 21:59–67
14. Fernandez X, Lizzani-Cuvelier L, Loiseau A, Perichet C, Delbecque C (2003) Volatile constituents of benzoin gums: Siam and Sumatra. Part 1. Flavour Fragr J 18:328–333
15. Eustis S, el-Sayed MA (2006) Why gold nanoparticles are more precious than pretty gold: noble metal surface plasmon resonance and its enhancement of the radiative and nonradiative properties of nanocrystals of different shapes. Chem Soc Rev 35:209–217
16. Magudapathy P, Gangopadhyay P, Panigrahi BK, Nair KGM, Dhara S (2001) Electrical transport studies of Ag nanoclusters embedded in glass matrix. Phys B 299:142–146
17. Kharat SN, Mendhulkar VD (2016) Synthesis, characterization and studies on antioxidant activity of silver nanoparticles using *Elephantopus scaber* leaf extract. Mater Sci Eng C Mater 62:719–724
18. Xue M, Zhang X, Wu ZF, Wang H, Ding X, Tian XY (2013) Preparation and flame retardancy of polyurethane/POSS nanocomposites. Chin J Chem Phys 26:445–450
19. Fan HB, Li XM, Liu YL, Yang RJ (2013) Thermal curing and degradation mechanism of polyhedral oligomeric octa(propargylaminophenyl)silsesquioxane. Polym Degrad Stabil 98:281–287
20. Baicea CM, Luntraru VI, Vaireanu DI, Vasile E, Trusca R (2013) Composite membranes with poly(ether ether ketone) as support and polyaniline like structure, with potential applications in fuel cells. Cent Eur J Chem 11:438–445
21. Jiang FY, Wang XD, Wu DZ (2014) Design and synthesis of magnetic microcapsules based on *n*-eicosane core and Fe_3O_4/SiO_2 hybrid shell for dual-functional phase change materials. Appl Energy 134:456–468
22. Guan B, Latif PA, Yap T (2013) Physical preparation of activated carbon from sugarcane bagasse and corn husk and its physical and chemical characteristics. Int J Eng Res Sci Technol 2:1–14
23. Yang HP, Yan R, Chen HP, Lee DH, Zheng CG (2007) Characteristics of hemicellulose, cellulose and lignin pyrolysis. Fuel 86:1781–1788
24. Rai M, Yadav A, Gade A (2009) Silver nanoparticles as a new generation of antimicrobials. Biotechnol Adv 27:76–83
25. Jakubovics NS, Kolenbrander PE (2010) The road to ruin: the formation of disease-associated oral biofilms. Oral Dis 16:729–739
26. Arunachalam KD, Arun LB, Annamalai SK, Arunachalam AM (2015) Potential anticancer properties of bioactive compounds of *Gymnema sylvestre* and its biofunctionalized silver nanoparticles. Int J Nanomed 10:31–41
27. Lin J, Huang ZH, Wu H, Zhou W, Jin PP, Wei PF, Zhang YJ, Zheng F, Zhang JQ, Xu J, Hu Y, Wang YH, Li YJ, Gu N, Wen LP (2014) Inhibition of autophagy enhances the anticancer activity of silver nanoparticles. Autophagy 10:2006–2020
28. Ahmed KBA, Mahapatra SK, Raja MRC, Subramaniam S, Sengan M, Rajendran N, Das SK, Haldar K, Roy S, Sivasubramanian A, Anbazhagan V (2016) Jacalin-capped silver nanoparticles minimize the dosage use of the anticancer drug, shikonin derivatives, against human chronic myeloid leukemia. Rsc Adv 6:18980–18989
29. Piao MJ, Kang KA, Lee IK, Kim HS, Kim S, Choi JY, Choi J, Hyun JW (2011) Silver nanoparticles induce oxidative cell damage in human liver cells through inhibition of reduced glutathione and induction of mitochondria-involved apoptosis. Toxicol Lett 201:92–100
30. Banerjee J, Narendhirakannan RT (2011) Biosynthesis of silver nanoparticles from *Syzygium cumini* (L.) seed extract and evaluation of their in vitro antioxidant activities. Dig J Nanomater Biosci 6:961–968
31. Babu S, Velez A, Wozniak K, Szydlowska J, Seal S (2007) Electron paramagnetic study on radical scavenging properties of ceria nanoparticles. Chem Phys Lett 442:405–408
32. Flora SJS (2007) Role of free radicals and antioxidants in health and disease. Cell Mol Biol 53:1–2
33. Niraimathi KL, Sudha V, Lavanya R, Brindha P (2013) Biosynthesis of silver nanoparticles using *Alternanthera sessilis* (Linn.) extract and their antimicrobial, antioxidant activities. Colloids Surf B Biointerfaces 102:288–291